



Título artículo / Títol article:

Organoselenium(II) halides containing the pincer 2,6-(Me₂NCH₂)₂C₆H₃ ligand – an experimental and theoretical investigation

Autores / Autors

Alexandra Pop, Anca Silvestru, Emilio José Juárez-Pérez, Massimiliano Arca, Vito Lippolis, Cristian Silvestru

Revista:

Dalton Transactions

Versión / Versió:

Post-print

Cita bibliográfica / Cita bibliogràfica (ISO 690):

POP, Alexandra, et al. Organoselenium (ii) halides containing the pincer 2, 6-(Me₂NCH₂)₂C₆H₃ ligand–an experimental and theoretical investigation. *Dalton Transactions*, 2014, vol. 43, no 5, p. 2221-2233.

url Repositori UJI:

<http://hdl.handle.net/10234/135625>

Organoselenium(II) halides containing the pincer
2,6-(Me₂NCH₂)₂C₆H₃ ligand – an experimental and
theoretical investigation†‡

Cite this: DOI: 10.1039/c3dt52886c

Alexandra Pop,^a Anca Silvestru,^a Emilio José Juárez-Pérez,^b Massimiliano Arca,^c
Vito Lippolis*^c and Cristian Silvestru*^a

New organoselenium(II) halides of the type [RSe]⁺X[−] [R = 2,6-(Me₂NCH₂)₂C₆H₃; X = Cl (**2**), Br (**3**), I (**4**)] were prepared by cleavage of the Se–Se bond in R₂Se₂ (**1**) with SO₂Cl₂ followed by halogen exchange when organoselenium chloride was treated with NaBr or KI. The reaction between **2** and R'₂MCl_{*n*} resulted in new ionic [RSe]⁺[R'₂MCl_{*n*}][−] [R' = 2-(Me₂NCH₂)C₆H₄, *n* = 1, M = Sb (**5**), Bi (**6**); R' = Ph, M = Sb, *n* = 1 (**7**) or *n* = 3 (**8**)] species. All new compounds were investigated in solution by multinuclear NMR spectroscopy (¹H, ¹³C, ⁷⁷Se, 2D experiments) and mass spectrometry. The ionic nature of **2** and the antimonates species was confirmed by conductivity studies. The molecular structures of [(2,6-(Me₂NCH₂)₂C₆H₃)Se]⁺Cl[−]·*n*H₂O (**2**·H₂O and **2**·2H₂O) and [(2,6-(Me₂NCH₂)₂C₆H₃)Se]⁺[Ph₂SbCl₄][−] (**8**), respectively, were established by single-crystal X-ray diffraction, pointing out that the ionic nature of these compounds is also preserved in the solid state, with both nitrogen atoms strongly *trans* coordinated to the selenium atom of the cation. Theoretical calculations carried out at the DFT level were exploited to investigate the nature of the bonding in compounds **2–4** and the free cation [RSe]⁺ (**2a**). A topological analysis based on the theory of Atoms-in-Molecules (AIM) and Electron Localization Function (ELF) jointly to a Natural Bond Orbital (NBO) approach was used to shed light on the effect of the nature of the halogen species X on the bonding within the 3c–4e N–Se–N moiety.

Received 13th October 2013,
Accepted 13th November 2013

DOI: 10.1039/c3dt52886c

www.rsc.org/dalton

^aDepartamentul de Chimie, Centrul de Chimie Supramoleculară Organică și Organometalică (CCSOOM), Facultatea de Chimie și Inginerie Chimică, Universitatea Babeș-Bolyai, RO-400028, Cluj-Napoca, Romania.

E-mail: cristian.silvestru@ubbcluj.ro; Fax: (+40) 264-590818; Tel: (+40) 264-593833

^bDepartment of Physics, Photovoltaic and Optoelectronic Devices Group, Universitat Jaume I, 12071 Castelló de la Plana, Spain

^cDipartimento di Scienze Chimiche e Geologiche, Università degli Studi di Cagliari, S.S. 554 Bivio per Sestu, 09042 Monserrato (CA), Italy. E-mail: lippolis@unica.it

†Dedicated to Professor Antonio Laguna (Universidad de Zaragoza, Spain) on the occasion of his 65th birthday.

‡Electronic supplementary information (ESI) available: Synthetic details for the preparation of **1**; crystal data and structure refinement for 2·H₂O, 2·2H₂O and **8** (Table S1); hydrogen bonds lengths and angles in the dimer association of 2·H₂O (Table S2); packing diagrams for 2·H₂O (Fig. S1–S3); selected bond distances and angles for the anion in **8** (Table S3); packing diagrams for **8** (Fig. S4–S6); stacked ⁷⁷Se NMR spectra (CDCl₃ r.t.) for **2**, **3**, and **4** (Fig. S7); Z-matrices of the optimized structures of **2a**, **2–4**, **2a'**, and **2'–4'**; selected optimized structural parameters for **2a** and **2–4** (Table S4); contribution of the main atomic orbital (AOs) to HOMOs and LUMOs calculated for **2a** and **2–4** (Table S5); isosurfaces of selected Kohn–Sham MOs calculated for **2a** and **2** (Fig. S8); calculated QTAIM parameters at the BCPs of the Se–C, Se–N, and Se–X bonds in **2a** and **2–4** (Table S6); core and valence shell population (number of electrons) from ELF of Se atom in compounds **2a** and **2–4** (Table S7); BCPs in the structure corresponding to the global and local minima from PES scan for **2** (Fig. S9) and corresponding relative electronic energy differences and energy interaction for the H...Cl bonds (Table S8); sum of the calculated electronic and thermal enthalpies and zero-point correction energies for **2a**, **2a'**, **2–4** and **2'–4'**, and relative enthalpies Δ*H*_f (Table S9). CCDC 952118–952120. For ESI and crystallographic data in CIF or other electronic format see DOI: 10.1039/c3dt52886c

Introduction

The chemistry of organoselenium compounds based on aromatic ligands bearing substituents which contain donor atoms able to provide intramolecular N–Se coordination raised considerable interest in recent years, mainly due to their applications in biology, asymmetric synthesis, catalysis or microelectronics.^{1–16} While one pendant arm ligands such as 2-(Me₂NCH₂)C₆H₄, 2-[E(CH₂CH₂)₂NCH₂]C₆H₄ (E = O, NMe), 2-(2'-oxazoliny)phenyl, 2-(RN=CH)C₆H₄ or related ones were quite often used in organoselenium chemistry, only a few compounds containing “pincer” aromatic groups have been reported.^{1,6} Examples include mainly organic groups with oxygen as a potential donor atom in the pendant arm, e.g. the diselenides such as [2,6-{EtOCH(Me)}₂C₆H₃]₂Se₂,¹⁷ [2,6-(MeOCH₂)₂-C₆H₃]₂Se₂,¹⁸ [4-^tBu-2,6-R₂C₆H₃]₂Se₂ [R = (CH₂O)₂CH, (O)CH, PhNH(O)C,¹⁹ MeO(O)C, ⁱPrO(O)C²⁰], or related mononuclear species as, for example, the selenides [2,6-{MeOCH(Me)}₂C₆H₃]-SeCH(Me)CH(Ph)[C₆H₂(OMe)_{3-2',4',6'}]²¹ or [4-^tBu-2,6-{MeO(O)C}₂-C₆H₃]₂SePh,²² the halide [4-^tBu-2,6-{MeO(O)C}₂-C₆H₃]₂SeBr²⁰ or [2,6-{MeOCH(Me)}₂C₆H₃]₂SeOTf.²¹ Compounds based on the asymmetric ligand 2-NO₂-6-(PhN=CH)C₆H₃ were also reported recently.²³ Organoselenium compounds containing (*N,C,N'*) “pincer” ligands are quite rare and limited to species bearing

the 2,6-(Me₂NCH₂)₂C₆H₃ on selenium. Furukawa and co-workers²⁴ reported the structural characterization of [2,6-(Me₂NCH₂)₂C₆H₃Se]⁺[PF₆]⁻, the first ionic species containing an organoselenium cation stabilized through two intramolecular N–Se interactions.³ This compound was obtained by reacting the selenides [2,6-(Me₂NCH₂)₂C₆H₃]SeR (R = Me, *n*-octyl) with ^tBuOCl followed by treatment with K[PF₆]. The dealkylation reaction leading to the same cation was also achieved by treatment of the above selenides with bromine. Later on, Poleschner and Seppelt¹⁸ reported that reaction of [2,6-(Me₂NCH₂)₂C₆H₃]₂Se₂ with XeF₂ in CH₂Cl₂ produced [2,6-(Me₂NCH₂)₂C₆H₃Se]⁺[HF₂]⁻ which could be converted by K[PF₆] into the same ionic species described by Furukawa. Recently, an X-ray diffraction study revealed the ionic nature of the organoselenium(II) bromide [2,6-(Me₂NCH₂)₂C₆H₃Se]⁺Br⁻·H₂O. The crystal contains dimers featuring two bromide anions, two cations, and two water molecules connected through Br...Se and Br...H interactions.²⁵

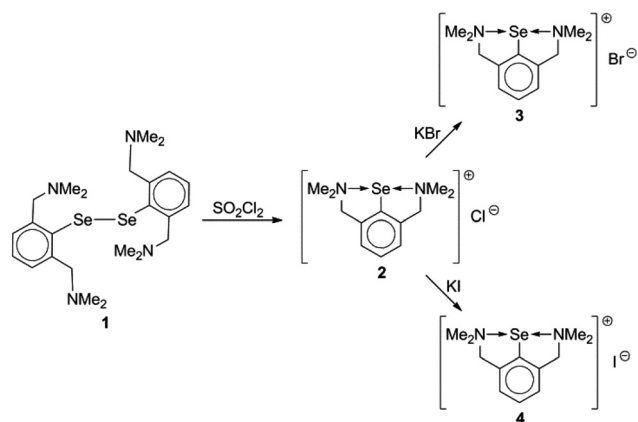
The importance of electrophilic selenium reagents, [ArSe]⁺X⁻, in the functionalization of olefins/acetylenes is well documented and several ionic species containing organoselenium cations, stabilized through intramolecular coordinating groups including “pincer” ligands, and noncoordinating anions were used.^{3,23}

As a part of our interest in organometallic compounds with (*N,C,N*) “pincer” ligands, herein we report on the synthesis and spectroscopic (NMR, MS) characterization of the several ionic species of the type [RSe]⁺X⁻ [R = 2,6-(Me₂NCH₂)₂C₆H₃; X = Cl (2), Br (3), I (4)] and [RSe]⁺[R'₂MCl_{*n*+1}]⁻ [R' = 2-(Me₂NCH₂)C₆H₄, *n* = 1, M = Sb (5), Bi (6); R' = Ph, M = Sb, *n* = 1 (7) or *n* = 3 (8)] as well as on the crystal and molecular structures of [2,6-(Me₂NCH₂)₂C₆H₃Se]⁺Cl⁻·*n*H₂O (2·H₂O and 2·2H₂O) and [2,6-(Me₂NCH₂)₂C₆H₃Se]⁺[Ph₂SbCl₄]⁻ (8). In order to better understand the N–Se–N three-body system in the free cation [RSe]⁺ (2a) and the effect of the halogen X in compounds 2–4, DFT theoretical investigations exploiting a topological analysis based on the theory of Atoms-In-Molecules (AIM) and Electron Localization Function (ELF) combined with a Natural Bond Orbital (NBO) approach were carried out.

Results and discussion

Synthesis

The diselenide [2,6-(Me₂NCH₂)₂C₆H₃]₂Se₂ (1) was prepared by a slight modification of the procedure previously reported by Poleschner and Seppelt,¹⁸ using ⁿBuLi instead of ^tBuLi for the *ortho* lithiation of 1,3-bis(dimethylaminomethyl)benzene, followed by insertion of elemental selenium into the newly formed carbon–lithium bond (see ESI[†]).^{8a} The cleavage of the Se–Se bond in 1 was achieved by treatment with SO₂Cl₂, at room temperature, in CCl₄ to give the ionic species [2,6-(Me₂NCH₂)₂C₆H₃Se]⁺Cl⁻ (2) as a pale yellow solid. The corresponding bromide 3 and iodide 4 were obtained from the chloride 2 and excess amounts of KBr and KI, respectively, in acetone at room temperature (Scheme 1).

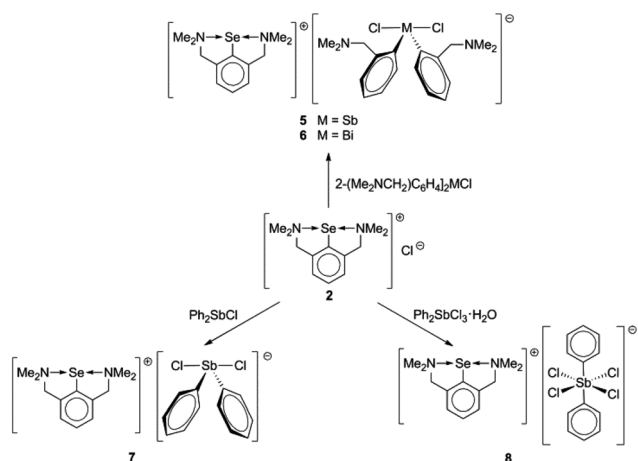


Scheme 1 Preparation of compounds 2–4.

It should be mentioned here that cleavage of the Se–Se bond in diselenide 1 could also be achieved with elemental bromine, and recrystallization in open atmosphere yielded the hydrate [2,6-(Me₂NCH₂)₂C₆H₃Se]⁺Br⁻·H₂O (3·H₂O), its structure having been already reported.²⁵ It is interesting to note that during attempts to purify the diselenide 1 from a dichloromethane–*n*-hexane mixture orange crystals of 2·2H₂O were isolated, probably formed as a result of the reaction with the halogenated solvent.

The ionic nature of 2 is reflected by its reactivity towards chlorides of the type R'₂MCl_{*n*} (M = Sb, Bi), the chloride ion being transferred to the pnictogen atom in acetonitrile, at room temperature. This results in new ionic species [RSe]⁺[R'₂MCl_{*n*+1}]⁻ [R' = 2-(Me₂NCH₂)C₆H₄, *n* = 1, M = Sb (5), Bi (6); R' = Ph, M = Sb, *n* = 1 (7) or *n* = 3 (8)] (Scheme 2). Such reactions between an onium halide and a diorganopnictogen(III) halide²⁶ or diorganoantimony(V) trihalide²⁷ are well documented.

All compounds were obtained as dioxygen stable, crystalline solids, which melt without decomposition. The chloride 2 is highly hygroscopic, a behaviour also suggested by its crystallization as hydrates with a different number of co-crystallized



Scheme 2 Preparation of compounds 5–8.

water molecules (see the subsequent discussion). The compounds are soluble in organic solvents, such as chloroform, methylene dichloride, acetonitrile or DMSO. MS and NMR data as well as elemental analytical data are consistent with the expected formulas. For all compounds 2–8 the ESI⁺ mass spectra constantly contain [2,6-(Me₂NCH₂)₂C₆H₃Se⁺] as the base peak. The conductivity of the chloride 2 and the antimonates 5, 7 and 8 in MeCN solutions is consistent with their ionic nature and formulation.

Solid state and solution behavior

Single-crystals of 2·H₂O and 8 were obtained by slow diffusion of *n*-hexane into a dichloromethane solution of the compounds, and their structures, as well as that of the dihydrate 2·2H₂O, were established by X-ray diffraction. The structures of 2·H₂O and 8 are shown in Fig. 1 and 2 and selected interatomic distances and bond angles in the [2,6-(Me₂NCH₂)₂C₆H₃Se]⁺ cation for all compounds are listed in Table 1.

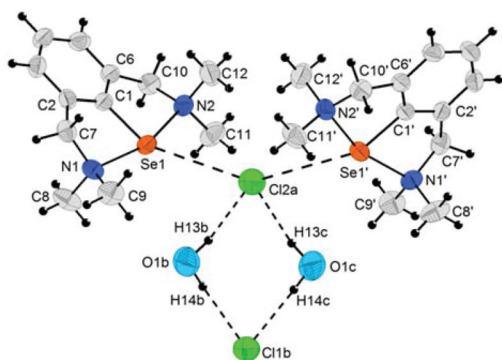


Fig. 1 Dimer association of (*R*_{N1},*R*_{N2})-cations in 2·H₂O, showing the atom numbering scheme. The atoms are drawn with 50% probability ellipsoids [symmetry equivalent atoms (1 - *x*, *y*, 1.5 - *z*), (-0.5 + *x*, 0.5 + *y*, *z*), (-0.5 + *x*, -0.5 + *y*, *z*) and (1.5 - *x*, -0.5 + *y*, 1.5 - *z*) are given by "prime", "a", "b" and "c", respectively].

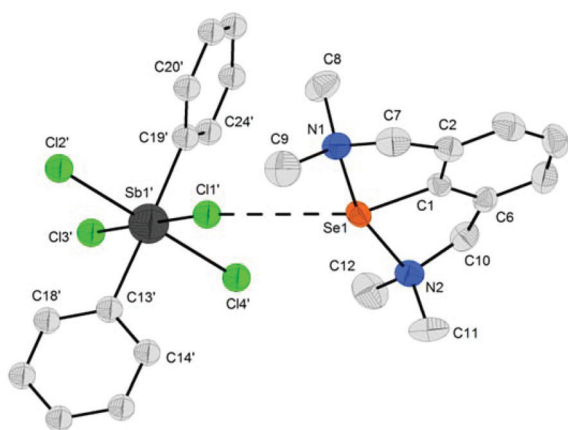


Fig. 2 Structure of ionic species 8, showing both the anion and the (*R*_{N1},*R*_{N2})-cation with the atom numbering scheme (hydrogen atoms are omitted for clarity). The atoms are drawn with 50% probability ellipsoids.

Table 1 Selected interatomic distances (Å) and angles (°) for the cation in 2·H₂O, 2·2H₂O and 8

	2·H ₂ O	2·2H ₂ O	8
C(1)–Se(1)	1.889(2)	1.883(3)	1.886(3)
N(1)–Se(1)	2.183(2)	2.175(3)	2.178(3)
N(2)–Se(1)	2.184(2)	2.177(3)	2.160(3)
N(1)–Se(1)–N(2)	161.31(8)	162.00(12)	161.95(11)
C(1)–Se(1)–N(1)	80.41(9)	81.09(15)	81.06(13)
C(1)–Se(1)–N(2)	81.04(9)	80.94(15)	81.02(13)

A common feature of compounds 2·*n*H₂O (*n* = 1, 2) and 8 is that the crystals contain [2,6-(Me₂NCH₂)₂C₆H₃Se]⁺ cations in which strong N–Se intramolecular interactions (see Table 1) [N–Se 2.183(2)/2.184(2) Å in 2·H₂O, 2.175(3)/2.177(3) Å in 2·2H₂O, and 2.160(3)/2.178(3) Å in 8] are established by both N atoms of the pendant arms, in *trans* positions to each other [N–Se–N 161.31(8)° in 2·H₂O, 162.00(12)° in 2·2H₂O, and 161.95(11)° in 8]. This results in a T-shaped (N,C,N)Se core (hypervalent 10-*Se*-3 species)²⁸ similar to what was observed in the cation of [2,6-(Me₂NCH₂)₂C₆H₃Se]⁺[PF₆]⁻ [N–Se 2.154/2.1840 Å; N–Se–N 161.90°]²⁴ or the related organoselenium(II) bromide [2,6-(Me₂NCH₂)₂C₆H₃Se]⁺Br⁻·H₂O [N–Se 2.181(3)/2.185(3) Å; N–Se–N 161.6(1)°].²⁵

The resulting five-membered SeNC₃ rings in the [2,6-(Me₂NCH₂)₂C₆H₃Se]⁺ cation are not planar, with the nitrogen atom lying above the best plane defined by the residual SeC₃ system. This induces planar chirality (with the aromatic ring and the nitrogen atom as the chiral plane and the pilot atom, respectively; for one five-membered ring the isomers are given as *R*_N and *S*_N, respectively)²⁹ and compounds 2·*n*H₂O (*n* = 1, 2) and 8 crystallize as racemates, *i.e.* 1:1 mixtures of (*R*_{N1},*R*_{N2}) and (*S*_{N1},*S*_{N2}) isomers (with respect to the two chelate rings in a cation unit).

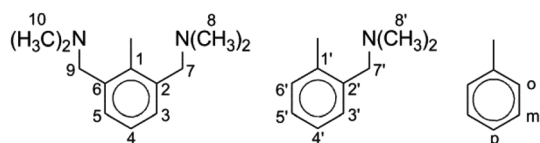
For 2·2H₂O, substitutional disorder of halogen and oxygen atoms (50% occupancy for Cl1/O1 and 0.50 for Cl2/O2, respectively) prevents any consideration concerning possible associations in the crystal based on hydrogen bonding or contacts with heavy atoms. However, the distance between selenium and a heavy atom is larger than 5.0 Å so that any interactions between cations and anions in the crystal of 2·2H₂O can be discounted. By contrast, the monohydrate 2·H₂O features a dimeric association (Fig. 1), with two isomer cations of the same chirality [either (*R*_{N1},*R*_{N2})/(*R*_{N1},*R*_{N2}) or (*S*_{N1},*S*_{N2})/(*S*_{N1},*S*_{N2})] bridged through one halide anion [Se(1)⋯Cl(2) 3.558(1) Å; Se(1)⋯Cl(2)⋯Se(1') 146.06(1)°; *cf.* ∑*r*_{cov}(Se,Cl) 2.16 Å, ∑*r*_{vdw}(Se,Cl) 3.81 Å^{30a}] of the (Cl⁻)₂(H₂O)₂ unit built on Cl⋯H interactions [Cl(2a)⋯H(13b) 2.24 Å; Cl(1b)⋯H(14b) 2.33 Å; *cf.* ∑*r*_{vdw}(Cl,H) 3.01 Å^{30a}]. A similar dimer association was shown to be present in the crystal of the analogous bromide 3·H₂O.²⁵ Chain polymers of alternating (*R*_{N1},*R*_{N2})/(*R*_{N1},*R*_{N2}) and (*S*_{N1},*S*_{N2})/(*S*_{N1},*S*_{N2}) dimer units are formed through further interaction C–H⋯π (Aryl_{centroid}) contacts (*i.e.* H⋯Ar_{centroid} contacts shorter than 3.1 Å, with an angle γ between the normal to the aromatic ring and the line defined by the H atom and Ar_{centroid} smaller than 30°),^{30b} C(7)–H(7Ah)_{methylene}⋯Ar_{centroid}{C(1)–C(6)}

2.92 Å, $\gamma = 11.4^\circ$. Additional weak Cl...H and O...H contacts result in a 3D architecture in the crystal of 2-H₂O (see for details Table S2, Fig. S1, S2a–c, S3a–c in the ESI†).

The coordination geometry around the antimony atom in the anion of **8** deserves no special comments. It is octahedral with the phenyl groups, placed in *trans* positions, basically bisecting the Cl–Sb–Cl angles of the square-planar SbCl₄ plane. The Sb–Cl bond distances fall within the range 2.4323(8)–2.4932(8) Å (see Table S3 in ESI†), as observed for other related ionic compounds.^{27g} They are of intermediate length between terminal and bridging antimony–halogen bonds in the dimer (Ph₂SbCl₃)₂ [2.346(4), 2.388(4) Å vs. 2.620(4), 2.839(4) Å].³¹ Weak Se...Cl contacts [3.680(1) Å] are established between cations and anions (Fig. 2). Dimer associations are formed between pairs of (*R*_{N1},*R*_{N2})-cation/Ph₂SbCl₄ and (*S*_{N1},*S*_{N2})-cation/Ph₂SbCl₄ based on C–H... π (Ph_{centroid}) contacts which involve one phenyl group of the anion [C(12)–H(12A)_{methyl}...Ph_{centroid}{C(13'a)–C(18'a)} 2.68 Å, $\gamma = 7.5^\circ$]. A layer of dimer cation–anion associations is built through anion–anion Cl...H interactions [Cl(3')...H(17c)_{phenyl} 2.87 Å] and C–H... π (Aryl_{centroid}) contacts between (*R*_{N1},*R*_{N2})- and (*S*_{N1},*S*_{N2})-cations [C(10)–H(10A)_{methylene}...Ar_{centroid}{C(1'b)–C(6'b)} 2.78 Å, $\gamma = 3.1^\circ$]. In the crystal of **8**, additional weak Cl...H and C–H... π (Aryl_{centroid}) contacts between layers result in 3D architectures (see for details Fig. S4, S5a,b, S6a–c in the ESI†).

The organoselenium compounds **1–8** were investigated in solution by multinuclear NMR spectroscopy (¹H, ¹³C, ⁷⁷Se) and the ¹H and ¹³C resonances were assigned based on 2D experiments, according to the numbering scheme illustrated in Scheme 3.

The room temperature NMR spectra of **1–8** exhibit only one set of resonances for the [2,6-(Me₂NCH₂)₂C₆H₃] group attached to the selenium atom suggesting that only one species is present in solution. Singlet ¹H and ¹³C signals were observed both for the methylene and methyl protons and carbons, respectively, indicating equivalence of the two pendant arms and a high symmetry of the cation on the NMR time scale due to a fast conformational change of the chelate five-membered SeC₃N rings. For compounds **5–8**, typical ¹H (sometimes overlapped) and ¹³C resonances were observed for the organic groups in the anion. In the case of **5** the spectra show broad ¹H resonances for the methyl and methylene protons in anion [2-[(Me₂NCH₂)₂C₆H₄]₂SbCl₂][−]. This pattern of the NMR spectra at room temperature suggests a fluxional behavior corresponding to the dissociation/re-coordination between the nitrogen atoms and the metal atom, with inversion at a three-coordinated nitrogen atom and rotation around the (H₂)C–N bond. A similar process was previously described for the starting material [2-(Me₂NCH₂)₂C₆H₄]₂SbCl.³²



Scheme 3 Numbering scheme for NMR assignments.

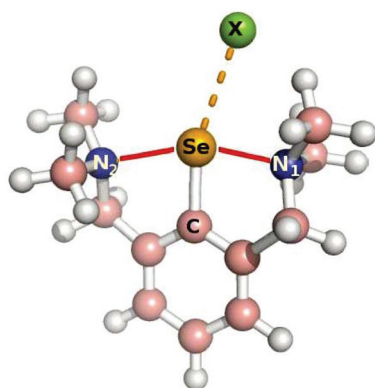
The ⁷⁷Se NMR spectra of compounds **2–8** are consistent with the formation of the ionic species. One singlet resonance is observed around δ 1200 ppm for these compounds, consistent with the presence of only one Se species in solution. The ⁷⁷Se resonances in **2–8** are strongly low-field shifted compared to the diorganodiselenide **1** (δ 395.6 ppm) used as the starting material to prepare the organoselenium(II) halides (see Fig. S7 in the ESI†). These values are in agreement with the values for analogous compounds described in the literature.^{8a,15}

Theoretical studies

Recently, we have reported on the synthesis and structural properties of organoselenium(II) halides of the type [2(Et₂NCH₂)C₆H₄]SeX (X = Cl, Br, I) featuring a three body system N→Se–X.^{16d} In particular, DFT calculations in the gas phase allowed to confirm a polarized 3c-4e nature for it with the entity of the N–Se intramolecular interaction decreasing on passing from X = Cl to X = I and the Se–X interaction correspondingly increasing. In **2–4**, the presence of a second N→Se intramolecular interaction to give a T-shaped (N,C,N)Se core results in a complete detachment of the halogen atom from the chalcogen centre with the formation of ionic organoselenium(II) compounds. In order to better establish the nature of the bond in **2–4** and the role played by the formation of the N→Se(C)←N hypervalent core in the ionicity of the title compounds we performed DFT calculations on the free cation [2,6-(Me₂NCH₂)₂C₆H₃]Se⁺ (**2a**) and on **2–4**. Furthermore, we also performed on the same systems a topological electron density analysis based on the quantum theory of atoms-in-molecules (QTAIM) approach and already applied with success to other types of hypervalent systems.³³

The geometries of **2a** and **2–4** were first optimized at the DFT level by using the LanL2DZ basis set with relativistic effective core potential, polarisation and diffuse functions for Se and halogen atoms (see the Experimental section and ESI†). An overall good match is observed between the calculated structural parameters for **2** and **3** and the corresponding experimental ones determined for 2-H₂O (see above) and 3-H₂O.²⁵ The highest discrepancy is observed for the Se–X distance. Furthermore, while the calculated Se–N₂ distance in **2** and **3** is slightly overestimated, the calculated Se–N₁ and Se–C distances are very close to the corresponding structural values (Scheme 4), the N₁–Se–N₂, X–Se–C and N₂–Se–C–C angles being also fairly well estimated. Interestingly, for each optimized halide **2–4** the two calculated Se–N distances are slightly different from each other and the difference becomes smaller on passing from X = Cl (**2**) to X = I (**4**). It is also important to point out that, in agreement with structural data of 2-H₂O, 2-2H₂O and **3**, in the optimized geometries of **2–4** the halide ions adopt a similar disposition with respect to the [RSe]⁺ cation as shown in Scheme 4. Selected optimized structural parameters for **2a** and **2–4** (Table S4†), and the Z-matrices of optimized structures have been deposited as ESI.†

An examination of the nature of Kohn–Sham (KS) HOMOs and LUMOs (Fig. 3 for **2a** and **2**) is in agreement with a slightly unbalanced 3c-4e nature for the N→Se(C)–N three-body system



Scheme 4 Optimized geometries for the $[RSe]^+X^-$ [$R = 2,6-(Me_2NCH_2)_2C_6H_3$] species [free cation (**2a**); $X = Cl$ (**2**), Br (**3**), I (**4**)].

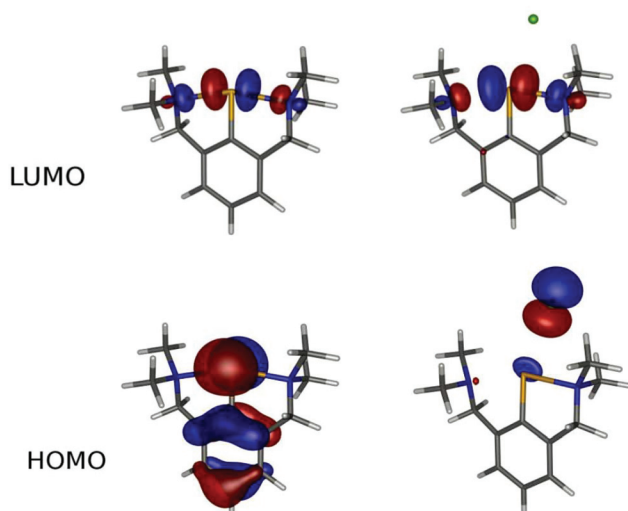


Fig. 3 Kohn-Sham HOMO and LUMO isosurfaces calculated for **2a** (left) and **2** (right). Contour value = 0.05 e.

in **2-4**, with the N atom of one pendant group acting as a donor towards the Se–N acceptor system formed by the N atom of the other pendant arm of the pincer ligand.

While in **2a** the HOMO is mainly formed by the $4p_z$ AO on the Se atom and $2p_z$ AOs from the C atoms of the aromatic ring (see Fig. 3), in **2-4** the HOMO is mainly localized on the halogen atoms consisting of a combination of mainly np_x and np_z AOs, although there is a small contribution from the Se atom mainly with the $4p_z$ AO and decreasing from $X = Cl$ (6.2%) to $X = I$ (2.7%). In all cases the HOMO is antibonding in character [see Table S5† for the contribution of main Atomic Orbitals (AOs) to the HOMOs and LUMOs in **2a** and **2-4**].

For all compounds, the LUMO shows a σ character along the N–Se–N axis due to the antibonding combination of $4p_x$ and $2p_x$ AOs from Se and N atoms, respectively.³⁴ Notably, the composition of this MO in terms of the constituent AOs corresponds to the antibonding $p\sigma$ combination of a $3c-4e$ system as described by the Rundle–Pimentel model (Fig. 3).³⁵ Also the

Table 2 Selected NBO charges and Wiberg bond indexes calculated for **2a** and **2-4**

		2a	2	3	4
NBO	Se	0.615	0.671	0.660	0.655
	N2	−0.532	−0.535	−0.534	−0.533
	N1	−0.532	−0.521	−0.523	−0.526
	C	−0.288	−0.306	−0.306	−0.306
	X	—	−0.834	−0.835	−0.845
Wiberg index	Se–N2	0.408	0.304	0.319	0.339
	Se–N1	0.409	0.448	0.438	0.425
	Se–C	0.997	0.960	0.956	0.955
	Se–X	—	0.1481	0.1480	0.1385

bonding and non-bonding MOs corresponding to the Rundle–Pimentel σ -bonding scheme primarily localized on the N–Se–N fragment can be envisaged among the calculated Kohn–Sham MOs (see Fig. S8† for **2a** and **2**).

On passing from $X = Cl$ (**2**) to $X = I$ (**4**), NBO analysis clearly indicates a progressive increase in the electronic population on the chalcogen atom that bears a positive charge, accompanied by a slight increase in the negative charge on N1 and the halogen centre. An examination of calculated Wiberg indexes for the Se–N bonds (Table 2) shows that, as deduced from the corresponding calculated bond lengths (Table S4†), on passing from $X = Cl$ (**2**) to $X = I$ (**4**) the entity of the Se–N2 interaction systematically increases while that of the Se–N1 interaction slightly decreases. The sum of the bond indexes calculated for the two Se–N bonds remains roughly constant, with a slight increase on passing from **2** to **4**, in agreement with a progressive strengthening of the N–Se–N three-body system. In the free cation **2a** the Wiberg indexes for the two Se–N bonds are equal. These trends are determined by the change in the halogen species, which are engaged in a remarkable ionic interaction with the Se center as supported by the trends in the calculated NBO negative charge on the halogens on passing from $X = Cl$ (**2**) to $X = I$ (**4**). However, on increasing the electronegativity of the halogen, some electron sharing between the Se atom and the halogen is calculated [see the trend in the Se–X WBIs on going from $X = Cl$ (**2**) to $X = I$ (**4**)], and therefore the degree of ionicity of these organoselenium(II) halides increases on going from Cl to I, which is accompanied by a balancing of the two N–Se interactions.

Overall, we can draw the same conclusions about the nature of the bond involving the Se atom in the compounds considered and the effects on the N→Se(C)←N system due to the presence of the halide species, by taking into account the electron population in the natural molecular orbitals involved in the chemical bonding of the hypervalent N→Se(C)←N moiety and the energy for the $n_N \rightarrow \sigma_{Se-N}^*$ delocalization interaction in compounds **2a** and **2-4** evaluated by the second order perturbation theory analysis of the Fock matrix in the NBO basis (Table 3). In particular, it is important to consider the increase in the amount of charge transferred from n_N MO to the antibonding MO (σ_{Se-N}^*) on passing from **2** to **4**, and the parallel increase in the $\Delta E^{(2)}_{n_N \rightarrow \sigma_{Se-N}^*}$ from 39.3 (**2**) to 46.99 (**4**), which reach the maximum value (59.45 kcal mol^{−1}) in the isolated

Table 3 Electron occupancy of the three valence NBOs $\sigma_{\text{Se-N}}$, $\sigma_{\text{Se-N}}^*$ and n_{N} , participating in the chemical bonding of the hypervalent N–Se(C)–N moiety in **2a**, **2–4**, and stabilization energy, $\Delta E^{(2)}(n_{\text{N}} \rightarrow \sigma_{\text{Se-N}}^*)$, due to electron delocalization from the donor to the acceptor NBOs

Compound	$\sigma_{\text{Se-N}}^*$	$\sigma_{\text{Se-N}}$	n_{N}	Total ^a	$\Delta E^{(2)}(n_{\text{N}} \rightarrow \sigma_{\text{Se-N}}^*)$ (kcal mol ⁻¹)
2a	0.34302	1.94844	1.64290	3.9344	59.45
2	0.30640	1.95118	1.70214	3.9597	39.53
3	0.31335	1.95034	1.69367	3.9574	42.65
4	0.32136	1.94899	1.68278	3.9534	46.99

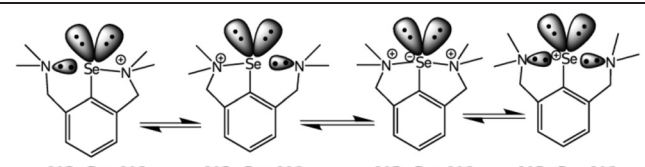
^aTotal electron occupancy: $\sigma_{\text{Se-N}} + \sigma_{\text{Se-N}}^* + n_{\text{N}}$.

RSe⁺ cation **2a**. The total occupancy of the three centers in the hypervalent N→Se(C)←N moiety is close to 4 electrons in all cases.

The theoretical data discussed so far clearly indicate that in the free cation **2a** a symmetric balanced 3c-4e system is present, which recalls other roughly linear different A–E–A systems featuring a central chalcogen species (E = S, Se) surrounded by two halogen or chalcogen A species.³⁶ The introduction of the halide X⁻ in **2–4** results in a progressive unbalancing of the N–Se–N moiety towards a N→Se–N system, which can be therefore envisaged as a charge-transfer (CT) system.

It is interesting to apply the recently developed Natural Resonance Theory (NRT) method to the hypervalent N–Se(C)–N moiety in **2a** and **2–4**, which offers a convenient and effective *ab initio* procedure to calculate candidate resonance structures and the corresponding weights.³⁷ According to the results reported in Table 4, the N–Se(C)–N moiety in **2a** and **2–4** can be described as roughly a 1 : 1 mixture of two resonance Lewis-type structures featuring each a single Se–N bond. In **2a** the contributions of the two structures (N2:Se–N1 and N2–Se:N1) to the resonance hybrid are identical and equal to 50%. In **2–4** the greatest contribution is calculated from the structure featuring, according to previous DFT calculations, the shortest Se–N bond (Table 4). The difference in the weight between the two N2:Se–N1 and N2–Se:N1 resonance structures decreases on passing from **2** to **4** and a decrease of the contribution from the limiting structure featuring two single Se–N bonds is

Table 4 Percentage weights of principal resonance structures calculated for the N–Se(C)–N moiety in **2a** and **2–4**



Compound	N2:Se–N1	N2–Se:N1	N2–Se–N1	N2:Se:N1
2a	50.0	49.7	0.3	0.0
2	57.7	40.7	1.6	0.0
3	56.3	42.2	1.5	0.0
4	54.5	44.3	1.2	0.0

observed from 1.6% to 1.2% on going from **2** to **4**. The limiting structure having no Se–N bonds has no contribution to the resonance hybrid in all cases.

With the aim of further investigating the nature of the chemical bonding in $[[2,6-(\text{Me}_2\text{NCH}_2)_2\text{C}_6\text{H}_3]\text{Se}]^+\text{X}^-$ we performed a topological electron density analysis on **2a** and **2–4** based on the quantum theory of atoms-in-molecules (QTAIM) approach developed by Bader (the calculated QTAIM properties at the bond critical points (BCPs) of the Se–C, Se–N and Se–X bonds for **2a** and **2–4** have been deposited in the ESI, Table S6[†]).^{38–42}

The QTAIM properties at the BCPs of the Se–C bonds are very similar in **2a** and **2–4** and in agreement with a covalent Se–C single bond picture as found for Se–C bonds in I–Se(C)–X hypervalent systems (X = I, Br, Cl).³³

As expected, the H^{38} value is negative at the BCPs of the Se–N bonds; however, the positive values for the calculated $\nabla^2\rho^{38}$ indicate an overall high polar covalent character for these bonds, in agreement with the very different NBO and QTAIM charges (Tables 2 and S6[†]) calculated on the Se and N atoms. Significantly, as observed for Wiberg's bond indexes, the difference between the values calculated for $\delta(\text{Se},\text{N}1)$ and $\delta(\text{Se},\text{N}2)^{38}$ decreases on going from **2** to **4** reaching the same value in **2a**, where the two Se–N bonds are balanced and are not affected by the presence of the halogenide ion. Furthermore, the sum of the $\delta(\text{Se},\text{N}1)$ and $\delta(\text{Se},\text{N}2)$ correlation indexes in **2a** and **2–4** is very close to the values found for $\delta(\text{Se},\text{C})$. Finally, the QTAIM properties at the BCPs of the Se–X bonds, especially the positive values calculated for H and the low positive values calculated for $\nabla^2\rho$, indicate an ionic or very polar nature for this interaction. Notably, the values of ρ and $\nabla^2\rho$ at the BCPs of the Se–X bond decrease on passing from **2** to **4** indicating, at least in the gas-phase, an increase in the polarity of this bond on passing from X = Cl to I.

Fig. 4 shows the localization basins calculated for the molecules **2a** and **2–4** by performing a topological analysis of the electron localization function (ELF).⁴³ Two well-separated monosynaptic valence $V(\text{Se})$ basins containing unshared valence electrons can be recognized around the selenium atom in each compound. In all cases, a distorted trigonal bipyramidal (tbp) disposition of the $V(\text{Se})$ and $V(\text{Se},\text{B})$ (B = N, C) disynaptic valence basins containing shared valence electrons around the selenium atom can be recognized. No disynaptic valence basins $V(\text{Se},\text{X})$ (X = Cl, Br, I) are found, indicating a basically ionic interaction between the halogenide ions and the **2a** cation.

The ELF analysis allows discriminating between core and valence basins and calculating the corresponding electron population, which is reported in Table S7.[†]

Whether or not the octet rule applies to hypervalent atoms in a three-body system is a matter of current debate,^{44a} and in this context the term hypercoordination has been proposed instead.^{44b,c} Notably, the Rundle–Pimentel view of 3c-4e bonds³⁵ does not require octet expansion.^{44d} Examination of the $N_v(\text{Se})$ values (number of electrons in the valence shell, shared and unshared) from ELF analysis for compounds **2a**

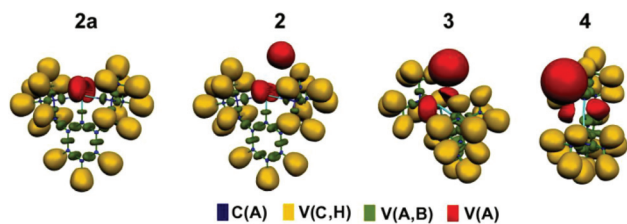


Fig. 4 Electron localization function (ELF) for **2a** and **2–4** (the isosurfaces include points at which the localization domain for the ELF is set equal to 0.82 for all molecules). C(A): core basins containing the core shell of electrons for each atom A; V(A,B): disynaptic valence basins containing valence electrons shared by two interacting atoms A and B and connecting the corresponding core basins; V(A): monosynaptic valence basins containing the unshared valence electrons around a given core basin C(A); the proton has no core electrons.

and **2–4** reveals that in all cases $N_v(\text{Se}) > 8$ and very close to 11, thus suggesting a hypervalent nature for the Se atom (Table S7†).

A number of valence shell electrons, $N_v(\text{Se})$, higher than 8 have been found in “T-shaped” compounds featuring 3c-4e I-Se(C)-X moieties (X = I, Br, Cl). In those cases, $N_v(\text{Se})$ ranges between 8.5 and 10.0 electrons, thus revealing a high donor capacity of the N atoms in the present N→Se(C)←N hypervalent systems and a high tendency to share their lone pair with the selenium centre in these compounds.³³

The fraction of electrons calculated within the disynaptic valence basins V(Se,X) (X = Cl, Br, I) is very low in agreement with an ionic nature of this bond, while the 3c-4e nature for the N→Se(C)←N system is confirmed by the number of electrons very close to 4 within the disynaptic valence basins V(Se,V) (Table S7†).

An intriguing structural aspect revealed by our calculations in the gas phase is the position of the halogenide anion with respect to the cation **2a**; in particular, the halogenide does not lie in the plane defined by the aromatic ring in the direction of the C–Se bond, but it is located closer to one of the N atoms (N1) forming a C–Se–X (X = Cl, Br, I) angle ranging from 159.0 (**2**) to 163.4° (**4**) and a C–C–Se–X dihedral angle ranging from 52.2 (**2**) to 64.8° (**4**) (Table 2). On the other hand, the crystal structures of the hydrated species **2**·H₂O, **2**·2H₂O, and **3**·H₂O confirm the capability of the halides to be differently oriented with respect to the **2a** unit, their relative positions being also determined by the extended network of hydrogen bonding interactions.

In order to understand the origin of the disposition of the halogenide anions with respect to the cation **2a** in the gas phase, a potential energy surface (PES) scan was therefore carried out by calculating the total electronic energy E for **2**, optimized for the C–Se–Cl angle and the Se–N–N–Cl and C–C–Se–Cl torsion angles in the range 150/210°, –140/120°, –180/180°, respectively. These three scans explore all possible chloride positions in the hemisphere above the cation **2a** and the results are shown in Fig. 5. The C–Se–Cl and C–C–Se–Cl scans give rise to two common global minima (yellow points in Fig. 5a and 5c) symmetrically disposed with respect to the

plane defined by the aromatic ring and, therefore, equivalent. The saddle points feature the chloride anion lying in the plane defined by the aromatic ring and forming a C–Se–Cl angle of 180° in the case of the C–Se–Cl scan. The Se–N–N–Cl scan features two minima, one of which (yellow point in Fig. 5b) corresponds to one of the two minima shared by the C–Se–Cl and C–C–Se–Cl scans for the position of the anion in the optimized structure. The other minimum (grey point in Fig. 5b) is 0.75 kcal mol^{–1} higher in energy and, therefore, should be considered a local minimum in the PES scan.

The geometry of **2** corresponding to the saddle point in the C–Se–Cl PES scan (C–Se–Cl = 180°) is characterized by an imaginary harmonic frequency calculated at –31 cm^{–1} and associated with the C–Se–Cl bending vibration and, therefore, it can be considered a transition state in the movement of the chloride ion from one side of the aromatic ring to the other side (green points in Fig. 5a and 5d) as confirmed by QST3 (Gaussian09, *Synchronous Transit-Guided Quasi-Newton Method*) analysis (see the Experimental section).

On the grounds of the results obtained from the PES scans we have considered the geometry of **2** in correspondence to the global and local minima found (yellow points in Fig. 5a–c and grey point in Fig. 5b) and in correspondence to the saddle point in Fig. 5a. In these structures, the chloride ion is involved in hydrogen bonds with the methyl groups from the amino pendant arms of the pincer ligand (Fig. S8†). We have evaluated the QTAIM parameters at the BCPs of all hydrogen bonds involving the Cl atom in these structures, which are typical of hydrogen bonding interactions. In particular, we have evaluated the energy interaction of each H...Cl bond using the Espinosa–Molins–Lacomte (EML) equation (Table S8†).⁴⁵ The sum of the H...Cl interaction energies for the considered structures indicates that intramolecular H...Cl interactions play a major role in determining the disposition of the chloride ion with respect to the cation **2a** in the ground state in the gas phase (see ESI† for a more detailed discussion).

In previous studies, the synthesis, characterization and electronic properties of organoselenium(II) compounds of the type [2-(R₂NCH₂)C₆H₄]₂SeX (R = Me, Et; X = Cl, Br, I) have been reported.^{15,16d} In these compounds a strong internal N→Se interaction is established in the solid state, thus resulting in a distorted T-shaped (C,N)SeX core with a polarized 3c-4e nature for the chemical bonding in the N→Se–X moiety. In the gas phase a progressive decrease of the N→Se interaction is calculated on going from X = Cl to X = I. In principle, neutral organoselenium(II) compounds of this kind featuring an N→Se–X moiety can also be formed starting from cation **2a** via substitution of one Me₂NCH₂ pendant arm at the selenium atom and coordination with a halide.

In order to quantify the relative stability of compounds **2–4** featuring the N→Se(C)←N hypervalent system (slightly unbalanced by the presence of the X[–] anion) with respect to compounds **2'–4'** featuring N→Se(C)–X moieties, the formation enthalpy of the species X[–], **2a**, **2a'**, **2–4** and **2'–4'** have been calculated. Hence, we have optimized the geometry of **2'–4'**

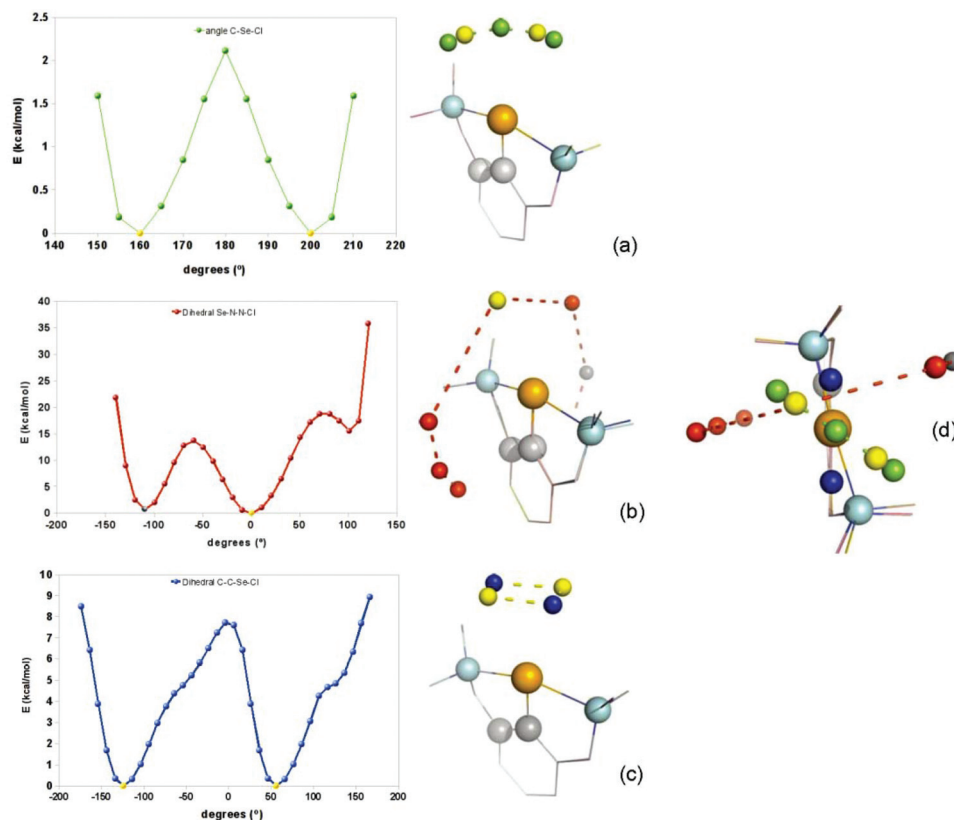


Fig. 5 PES scans calculated for **2** at the DFT level on varying (a) the C–Se–Cl angle, (b) the Se–N–N–Cl, and (c) C–C–Se–Cl dihedral angles in the range 150/210°, –140/120°, –180/180°, respectively; (d) top view of the three performed PES scans together.

(see ESI[†]) and calculated the formation enthalpy of the cation species **2a** and **2a'** by considering the equation $[\text{RSe}]^+ + \text{X}^- \rightarrow \text{RSeX}$ [$\Delta H_f(2a/2a') = \Delta H_f(2-4/2'-4') - \Delta H_f(\text{X}^-)$]. The results are summarized in Table S9 (ESI[†]).

Interestingly, compounds **2'–4'**, featuring only one N→Se interaction and the N→Se–X framework, are thermodynamically more stable than the corresponding compounds **2–4** featuring the N–Se(C)–N hypervalent moiety by about 4 kcal mol^{–1}. In contrast, the **2a** cation is much more stable than the **2a'** cation by 25.5 kcal mol^{–1} (see Fig. 6). This justifies the absence of **2–4** to **2'–4'** inter-conversions in solution as demonstrated by NMR measurements. This interconversion in fact would require an initial high energy cost to break one of the two N–Se interactions.

Conclusions

Compounds of the type $[\{2,6-(\text{Me}_2\text{NCH}_2)_2\text{C}_6\text{H}_3\}\text{Se}]^+ \text{X}^-$ [X = Cl (**2**), Br (**3**), I (**4**)] have been synthesized starting from the diselenide $[2,6-(\text{Me}_2\text{NCH}_2)_2\text{C}_6\text{H}_3]_2\text{Se}_2$ (**1**). The novel compounds have been fully characterized by spectroscopic means and compounds **2·H₂O**, **2·2H₂O**, and $[\{2,6-(\text{Me}_2\text{NCH}_2)_2\text{C}_6\text{H}_3\}\text{Se}]^+[\text{Ph}_2\text{SbCl}_4]^-$ (**8**) have been characterized by single-crystal X-ray diffraction analysis. The structural and spectroscopic characterization suggests the N–Se–N moiety as a 3c-4e system.

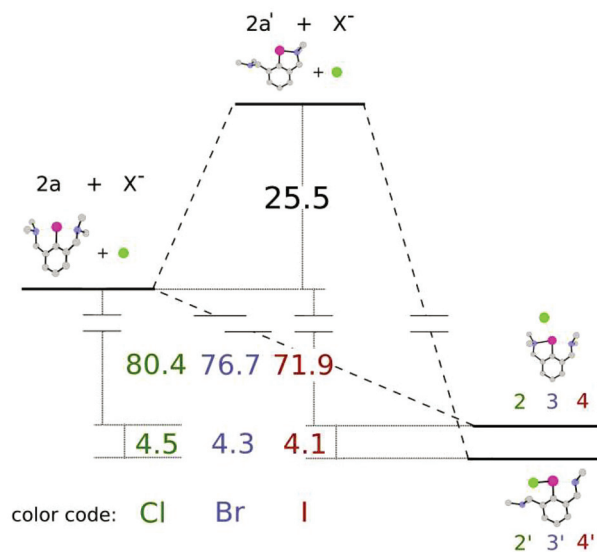


Fig. 6 Enthalpy of formation (ΔH_f^{298} , kcal mol^{–1}) for compounds **2–4** starting from **2a**, and for compounds **2'–4'** starting from **2a** via the intermediate cation **2a'**.

In this context, an in-depth theoretical investigation at the DFT level was carried out. The geometries of compounds **2–4** have been optimized and the potential energy surface (PES) has been explored in order to ascertain the possible position

of the anion X^- with respect to the cation $[\{2,6-(\text{Me}_2\text{NCH}_2)_2\text{C}_6\text{H}_3\}\text{Se}]^+$ (**2a**). Overall, DFT calculations show that the N–Se–N system can be envisaged as a strongly polarized 3c-4e three-body system. Accordingly, the KS-LUMO is clearly represented by the antibonding σ -combination of atomic orbitals as described by the Rundle–Pimentel bonding scheme. The nature of the X^- halide is reflected in an unbalancing of the N–Se–N system towards a charge-transfer N→Se–N system on passing from **4** to **2**. This conclusion is supported by the calculation of Wiberg bond indexes and NBO calculations. Further calculations, carried out within the framework of Bader's quantum theory of atoms-in-molecules (QTAIM), confirm the polarized nature of N–Se bonds in **2–4**. The topological analysis of the electron localized function (ELF) supports a hypervalent nature of the Se atom. Notably, a comparison of the AIM parameters calculated for the N–Se–N system of **2a/2–4** and I–Se(C)–X systems (X = Cl, Br, I) featured by T-shaped dihalogen adducts of selenocarbonyl donors shows similar values for both three-body systems, providing a further example of how apparently different chemical systems can share similar bonding nature. This confirms the suggestive conclusions derived from a recent structural survey on A–B–C systems containing different combinations of halogen and chalcogen species embedded within charge-transfer and T-shaped hypervalent systems,³⁶ which share a common correlation between the A–B and B–C bond distances accountable by means of the bond-valence model.

Experimental section

General procedures

The ^1H , ^{13}C and ^{77}Se NMR spectra were recorded in CDCl_3 and DMSO solutions at room temperature on a Bruker AVANCE 300 instrument operating at 300.11, 75.46 and 57.24 MHz, respectively. The ^1H chemical shifts are reported in δ units (ppm) relative to the residual peak of the deuterated solvent (ref. CHCl_3 : ^1H 7.26 ppm; DMSO- d_6 : ^1H 2.50 ppm). The ^{13}C chemical shifts are reported in δ units (ppm) relative to the peak of the solvent (ref. CHCl_3 : ^{13}C 77.0 ppm; DMSO- d_6 : ^{13}C 39.43 ppm). ^1H and ^{13}C resonances were assigned using 2D NMR experiments (COSY, HSQC and HMBC) which were performed using standard pulse sequences in the version with z-gradients, as delivered by Bruker with TopSpin 1.3 PL6 spectrometer control and processing software. The ^{77}Se spectra were obtained using diphenyldiselenide as an external standard. Chemical shifts are reported relative to dimethylselenide (δ 0 ppm) by assuming that the resonance of Ph_2Se_2 is at δ 461 ppm.⁴⁶ The NMR spectra were processed using the *MestReC* and *MestReNova* software.⁴⁷ The ESI^+ mass spectra were recorded using an Esquire 3000 ion-trap mass spectrometer (Bruker Daltonic GmbH) and a Thermo Scientific LTQ Orbitrap XL mass spectrometer. Samples were introduced by direct infusion with a syringe pump. Nitrogen served both as the nebulizer gas and the dry gas. Helium served as a cooling gas for the ion trap and a collision gas for MS_n experiments. Conductivity

measurements of 10^{-4} M solutions in acetonitrile (HPLC grade) were performed at 25 °C using a Bench Conductivity/TDS Meter CON 510 instrument containing 2-ring stainless steel Ultem-body Conductivity/TDS electrode (cell constant $K = 1.0$) with a built-in temperature sensor (EC-CONSEN 91W/35608-50). Melting points were measured with an Electrothermal 9200 apparatus and are not corrected. Elemental analyses were carried out with a CHN-Analysator Type FlashAE 1112 (Co. Thermo) instrument. Solvents were dried and freshly distilled under argon prior to use. The starting materials, 1,3- $(\text{Me}_2\text{NCH}_2)_2\text{C}_6\text{H}_4$,⁴⁸ Ph_2SbCl ,⁴⁹ $\text{Ph}_2\text{SbCl}_3 \cdot \text{H}_2\text{O}$,⁵⁰ $[2-(\text{Me}_2\text{NCH}_2)\text{C}_6\text{H}_4]_2\text{SbCl}$,³² and $[2-(\text{Me}_2\text{NCH}_2)\text{C}_6\text{H}_4]_2\text{BiCl}$,⁵¹ were prepared according to literature methods. The reagents SO_2Cl_2 , KBr, KI and $^n\text{BuLi}$ were purchased from Sigma Aldrich and used without further purification.

Synthesis of $[\{2,6-(\text{Me}_2\text{NCH}_2)_2\text{C}_6\text{H}_3\}\text{Se}]^+\text{Cl}^-$ (2**).** A solution of **1** (1.76 g, 3.26 mmol) in CCl_4 (30 mL) was treated dropwise with a solution of SO_2Cl_2 (0.44 g, 3.26 mmol) in CCl_4 (20 mL). The reaction mixture was stirred at room temperature for 24 h. Then the resulting solid product was filtered off, dissolved in CH_2Cl_2 and the organic solution was washed with a saturated solution of KOH. The organic phase was separated, and dried over Na_2SO_4 , and removal of the solvent *in vacuo* gave **2** (1.45 g, 73%) as a pale yellow solid, m.p. 106 °C. Anal. calcd for $\text{C}_{12}\text{H}_{19}\text{ClN}_2\text{Se}$ (305.71): C 47.15, H 6.26, N 9.16; Found: C 47.35, H 6.28, N 9.10%. Λ_M 344 $\Omega^{-1} \text{cm}^2 \text{mol}^{-1}$. ^1H NMR (CDCl_3): δ 2.94 (12 H, s, H-8,10, CH_3), 4.14 (4 H, s, H-7,9, CH_2), 7.32 (3 H, m, H-3,4,5, C_6H_3). ^{13}C NMR (CDCl_3): δ 48.81 (s, C-8,10, CH_3), 63.92 (s, C-7,9, CH_2), 125.86 (s, C-3,5), 128.40 (s, C-4), 132.29 (s, C-2,6), 132.46 (s, C-1). ^{77}Se NMR (CDCl_3): δ 1202.2 (s). MS (ESI^+), m/z (%): 271 $[\{2,6-(\text{Me}_2\text{NCH}_2)_2\text{C}_6\text{H}_3\}\text{Se}]^+$.

Synthesis of $[\{2,6-(\text{Me}_2\text{NCH}_2)_2\text{C}_6\text{H}_3\}\text{Se}]^+\text{Br}^-$ (3**).** A solution of **2** (0.500 g, 1.64 mmol) in acetone (30 mL) was treated dropwise with a solution of KBr (0.380 g, 3.19 mmol) in acetone (20 mL). The reaction mixture was stirred at room temperature for 24 h and then filtered and removal of the solvent from the clear solution gave **3** (0.47 g, 83%) as a pale orange solid, m.p. 143 °C. Anal. calcd for $\text{C}_{12}\text{H}_{19}\text{BrN}_2\text{Se}$ (350.16): C 41.16, H 5.47, N 8.00; Found: C 41.21, H 5.49, N 7.97%. ^1H NMR (CDCl_3): δ 3.06 (12 H, s, H-8,10, CH_3), 4.19 (4 H, s, H-7,9, CH_2), 7.31 (3 H, m, H-3,4,5, C_6H_3). ^{13}C NMR (CDCl_3): δ 49.33 (s, C-8,10, CH_3), 64.35 (s, C-7,9, CH_2), 125.97 (s, C-3,5), 128.47 (s, C-4), 132.11 (s, C-2,6), 132.75 (s, C-1). ^{77}Se NMR (CDCl_3): δ 1211.2 (s). MS (ESI^+), m/z (%): 271 $[\{2,6-(\text{Me}_2\text{NCH}_2)_2\text{C}_6\text{H}_3\}\text{Se}]^+$.

Synthesis of $[\{2,6-(\text{Me}_2\text{NCH}_2)_2\text{C}_6\text{H}_3\}\text{Se}]^+\text{I}^-$ (4**).** Prepared as described for **3** from **2** (0.500 g, 1.64 mmol) and KI (0.540 g, 3.25 mmol) in acetone (50 mL). Work-up of the reaction mixture gave **4** (0.55 g, 85%) as a pale yellow solid, m.p. 216 °C. Anal. calcd for $\text{C}_{12}\text{H}_{19}\text{IN}_2\text{Se}$ (397.16): C 36.29, H 4.82, N 7.05; Found: C 36.29, H 4.52, N 6.98%. ^1H NMR (CDCl_3): δ 3.03 (12 H, s, H-8,10, CH_3), 4.22 (4 H, s, H-7,9, CH_2), 7.31 (3 H, m, H-3,4,5, C_6H_3). ^{13}C NMR (CDCl_3): δ 49.10 (s, C-8,10, CH_3), 64.19 (s, C-7,9, CH_2), 125.95 (s, C-3,5), 128.47 (s, C-4), 132.34 (s, C-2,6), 132.75 (s, C-1). ^{77}Se NMR (CDCl_3): δ 1206.5 (s). MS (ESI^+), m/z (%): 271 $[\{2,6-(\text{Me}_2\text{NCH}_2)_2\text{C}_6\text{H}_3\}\text{Se}]^+$.

Synthesis of $[[2,6-(\text{Me}_2\text{NCH}_2)_2\text{C}_6\text{H}_3]\text{Se}]^+[2-\{(\text{Me}_2\text{NCH}_2)_2\text{C}_6\text{H}_4\}_2\text{SbCl}_2]^-$ (5). A solution of $[2-(\text{Me}_2\text{NCH}_2)_2\text{C}_6\text{H}_4]_2\text{SbCl}$ (0.139 g, 0.33 mmol) in acetonitrile (20 mL) was added dropwise to a stirred solution of **2** (0.100 g, 0.33 mmol) in acetonitrile (15 mL). The reaction mixture was stirred for 24 h and then the solvent was removed *in vacuo* to give **5** (0.21 g, 87%) as a yellow powder, m.p. 103 °C. Anal. calcd for $\text{C}_{30}\text{H}_{43}\text{Cl}_2\text{N}_4\text{SbSe}$ (731.32): C 49.27, H 5.93, N 7.66; Found: C 49.25, H 5.90, N 7.58%. Λ_{M} 203 $\Omega^{-1} \text{ cm}^2 \text{ mol}^{-1}$. ^1H NMR (CDCl_3): δ 2.26 (12 H, s, br, H-8', CH_3), 2.97 (12 H, s, H-8,10, CH_3), 3.68 (4 H, s, br, H-7', CH_2), 4.17 (4 H, s, H-7,9, CH_2), 7.18–7.33 (9 H, m, H-3',4',5' + H-3,4,5, C_6H_4 + C_6H_3), 7.84 (2 H, s, br, H-6', C_6H_4). ^{77}Se NMR (CDCl_3): δ 1202.4 (s). MS (ESI^+), m/z (%): 271 $[2,6-(\text{Me}_2\text{NCH}_2)_2\text{C}_6\text{H}_3\text{Se}^+]$.

Synthesis of $[[2,6-(\text{Me}_2\text{NCH}_2)_2\text{C}_6\text{H}_3]\text{Se}]^+[2-\{(\text{Me}_2\text{NCH}_2)_2\text{C}_6\text{H}_4\}_2\text{BiCl}_2]^-$ (6). Prepared as described for **5** from **2** (0.100 g, 0.33 mmol) and $[2-(\text{Me}_2\text{NCH}_2)_2\text{C}_6\text{H}_4]_2\text{BiCl}$ (0.169 g, 0.33 mmol) in acetonitrile (30 mL). Work-up of the reaction mixture gave **6** (0.234 g, 87%) as a yellow powder, m.p. 110 °C. Anal. calcd for $\text{C}_{30}\text{H}_{43}\text{BiCl}_2\text{N}_4\text{Se}$ (818.54): C 44.02, H 5.29, N 6.84; Found: C 44.21, H 5.38, N 6.82%. ^1H NMR (CDCl_3): δ 2.36 (12 H, s, H-8', CH_3), 2.84 (12 H, s, H-8,10, CH_3), 3.74 (4 H, s, H-7', CH_2), 4.05 (4 H, s, H-7,9, CH_2), 7.22 (3 H, m, H-3,4,5, C_6H_3), 7.38 (4 H, m, H-4',5', C_6H_4), 7.49 (2 H, d, H-3', C_6H_4 , $^3J_{\text{HH}}$ 7.0 Hz), 8.52 (2 H, d, H-6', C_6H_4 , $^3J_{\text{HH}}$ 6.9 Hz). ^{13}C NMR (CDCl_3): δ 45.89 (s, C-8', CH_3), 48.78 (s, C-8,10, CH_3), 63.88 (s, C-7,9, CH_2), 67.93 (s, C-7', CH_2), 125.81 (s, C-3,5), 128.00 (s, C-4'), 128.16 (s, C-4), 129.67 (s, C-3'), 130.98 (s, C-5'), 139.47 (s, C-6'), 132.32 (s, C-2,6), 132.50 (s, C-1), 145.95 (s, C-2'), 183.95 (s, C-1'). ^{77}Se NMR (CDCl_3): δ 1202.2 (s). MS (ESI^+), m/z (%): 271 $[2,6-(\text{Me}_2\text{NCH}_2)_2\text{C}_6\text{H}_3\text{Se}^+]$.

Synthesis of $[[2,6-(\text{Me}_2\text{NCH}_2)_2\text{C}_6\text{H}_3]\text{Se}]^+[\text{Ph}_2\text{SbCl}_2]^-$ (7). Prepared as described for **5** from **2** (0.100 g, 0.33 mmol) and Ph_2SbCl (0.103 g, 0.33 mmol) in acetonitrile (35 mL). Work-up of the reaction mixture gave **7** (0.174 g, 85%) as a yellow powder, m.p. 239 °C. Anal. calcd for $\text{C}_{24}\text{H}_{29}\text{Cl}_2\text{N}_2\text{SbSe}$ (617.13): C 46.71; H 4.74, N 4.54; Found: C 46.80, H 4.78, N 4.50%. Λ_{M} 312 $\Omega^{-1} \text{ cm}^2 \text{ mol}^{-1}$. ^1H NMR (CDCl_3): δ 2.66 (12 H, s, H-8,10, CH_3), 3.82 (4 H, s, H-7,9, CH_2), 7.08–7.23 (9 H, m, H-3,4,5 + H-*meta* + *para*, C_6H_3 + C_6H_5), 8.00 (4 H, s, br, H-*ortho*, C_6H_5). ^{13}C NMR (CDCl_3): δ 45.55 (s, C-8,10, CH_3), 63.65 (s, C-7,9, CH_2), 125.72 (s, C-3,5), 127.65 (s, C-*para*), 127.79 (s, C-*meta*), 128.24 (s, C-4), 131.99 (s, C-2,6), 132.23 (s, C-1), 135.87 (s, C-*ortho*), 149.91 (s, C-*ipso*). ^{77}Se NMR (CDCl_3): δ 1202.7 (s). MS (ESI^+), m/z (%): 271 $[2,6-(\text{Me}_2\text{NCH}_2)_2\text{C}_6\text{H}_3\text{Se}^+]$.

Synthesis of $[[2,6-(\text{Me}_2\text{NCH}_2)_2\text{C}_6\text{H}_3]\text{Se}]^+[\text{Ph}_2\text{SbCl}_4]^-$ (8). Prepared as described for **5** from **2** (0.060 g, 0.20 mmol) and $\text{Ph}_2\text{SbCl}_3 \cdot \text{H}_2\text{O}$ (0.080 g, 0.20 mmol) in acetonitrile (40 mL). Work-up of the reaction mixture gave **8** (0.112 g, 81%) as a yellow powder. The title compound was recrystallized from acetonitrile to give yellow crystals, m.p. 191 °C. Anal. calcd for $\text{C}_{24}\text{H}_{29}\text{Cl}_4\text{N}_2\text{SbSe}$ (688.04): C 41.90, H 4.25, N 4.07; Found: C 42.01, H 4.29, N 4.02%. Λ_{M} 157 $\Omega^{-1} \text{ cm}^2 \text{ mol}^{-1}$. ^1H NMR ($\text{DMSO}-d_6$): δ 2.79 (12 H, s, H-8,10, CH_3), 4.08 (4 H, s, H-7,9, CH_2), 7.27–7.32 (3 H, m, H-3,4,5, C_6H_3), 7.52–7.64 (6 H, m, H-*meta* + *para*, C_6H_5), 8.09 (4 H, d, H-*ortho*, C_6H_5 , $^3J_{\text{HH}}$ 7.4 Hz).

^{13}C NMR ($\text{DMSO}-d_6$): δ 48.19 (s, C-8,10, CH_3), 63.03 (s, C-7,9, CH_2), 125.52 (s, C-3,5), 128.04 (s, C-4), 128.75 (s, C-*para*), 129.89 (s, C-*meta*), 130.90 (s, C-2,6), 131.87 (s, C-*ipso*), 133.07 (s, C-1), 133.59 (s, C-*ortho*). ^{77}Se NMR ($\text{DMSO}-d_6$): δ 1187.6 (s). MS (ESI^+), m/z (%): 271 $[2,6-(\text{Me}_2\text{NCH}_2)_2\text{C}_6\text{H}_3\text{Se}^+]$.

Crystal structure

The crystals were mounted with epoxy glue on cryoloops and the data were collected with a Bruker SMART APEX diffractometer by using graphite-monochromated Mo-K α radiation ($\lambda = 0.71073 \text{ \AA}$) at room temperature (297 K). The structures were refined with anisotropic thermal parameters. The hydrogen atoms were refined with a riding model and a mutual isotropic thermal parameter. For structure solving and refinement the software package SHELX-97 was used.⁵² Compound $2 \cdot 2\text{H}_2\text{O}$ was refined as substitutional disorder of halogen and oxygen atoms with 0.50 occupancy for Cl1/O1 and 0.50 for Cl2/O2. The drawings were created with the Diamond program.⁵³ Additional crystallographic data are summarized in Table S1.†

Theoretical calculations

Quantum chemical DFT calculations were performed on **2a**, **2a'**, **2-4** and **2'-4'** structures using the commercial suite Gaussian 09 (Rev. B.01),⁵⁴ with Adamo and Barone's mPW1PW functional.⁵⁵ Although the use of all-electron basis sets provides better accuracy, pseudo-potential techniques are useful when relativistic effects must be taken into account. Thus, the double- ζ plus polarisation all-electron (pVDZ) basis set by Horn, Schafer and Ahlrichs for C, H, and N,⁵⁶ and the LANL2DZdp basis sets with relativistic core potentials, polarisation and diffuse functions for Se and halogen atoms were adopted.^{57,58} Vibrational analyses were used to check the nature of the stationary points and none of the optimised geometries presented imaginary frequencies at the DFT level unless otherwise specified in the text. From these frequency calculations, theoretical gas-phase enthalpy changes were obtained for the above compounds and Cl^- , Br^- and I^- ions at the same level of theory to evaluate the relative stability of cations **2a** and **2a'**. Mulliken charges were obtained from Gaussian 09 calculations, NPA charges were calculated using NBO Version 5.0⁵⁹ and QTAIM (Bader) charges from the software package AIMAll.⁶⁰ Wiberg 2-center indexes were calculated using NBO Version 5.0, 2-center delocalisation indexes in the framework of the QTAIM [$\delta(\text{A},\text{B})$] are obtained from AIMAll,⁶⁰ and 3-center indexes [$\delta(\text{A},\text{B},\text{C})$] from WBader.⁶¹ Analysis of the atomic orbital (AOs) contributions to the HOMO and LUMO from the "Mulliken routine" of Multiwfn 2.5.⁶² Second-order analysis of the Fock matrix energies and NRT results were obtained using NBO Version 5.0. Topological analysis in the framework of the QTAIM was done using AIMAll at the same level of theory.⁶³ The analysis of the ELF function was carried out with TopMod^{64,65} using all-electron densities and the ELF isosurfaces were visualised with Molekel.⁶⁶ HOMO and LUMO isosurfaces were obtained using Gabedit 2.4.0⁶⁷ and the

1 figures from scans and QST3 calculations were obtained using
PyMOL.⁶⁸

5 Acknowledgements

Financial support from the National University Research
Council of Romania (research projects PN-II-ID-PCE-2011-3-
0659 and PN-II-ID-PCE-2011-3-0933) is greatly appreciated. We
10 also thank the NATIONAL CENTER FOR X-RAY DIFFRACTION
(Babes-Bolyai University, Cluj-Napoca, Romania) for the
support with the solid state structure determinations and the
University of Cagliari for financial support.

15 Notes and references

- 1 G. Mugesh and H. B. Singh, *Chem. Soc. Rev.*, 2000, **29**, 347.
- 2 *Organoselenium Chemistry: Modern Developments in Organic
Synthesis, Topics in Current Chemistry*, ed. T. Wirth,
Springer, Berlin, 2000, vol. 208.
- 3 N. Furukawa, K. Kobayashi and S. Sato, *J. Organomet.
Chem.*, 2000, **611**, 116 and references therein.
- 4 G. Mugesh, W.-W. du Mont and H. Sies, *Chem. Rev.*, 2001,
25 **101**, 2125 and references therein.
- 5 G. Mugesh and H. B. Singh, *Acc. Chem. Res.*, 2002, **35**, 226.
- 6 A. J. Mukherjee, S. S. Zade, H. B. Singh and R. B. Sunoj,
Chem. Rev., 2010, **110**, 4357 and references therein.
- 7 (a) M. Iwaoka and S. Tomoda, *J. Am. Chem. Soc.*, 1996, **118**,
8077; (b) M. Iwaoka, H. Komatsu, T. Katsuda and
S. Tomoda, *J. Am. Chem. Soc.*, 2004, **126**, 5309.
- 8 (a) R. Kaur, H. B. Singh and R. P. Patel, *J. Chem. Soc.,
Dalton Trans.*, 1996, 2719; (b) A. Panda, G. Mugesh,
35 H. B. Singh and R. J. Butcher, *Organometallics*, 1999, **18**,
1986; (c) G. Mugesh, A. Panda, H. B. Singh and
R. J. Butcher, *Chem.–Eur. J.*, 1999, **5**, 1411; (d) G. Mugesh,
A. Panda, S. Kumar, S. D. Apte, H. B. Singh and
R. J. Butcher, *Organometallics*, 2002, **21**, 884; (e) G. Mugesh,
40 A. Panda, H. B. Singh, N. S. Punekar and R. J. Butcher,
J. Am. Chem. Soc., 2001, **123**, 839; (f) S. Kumar, K. Kandasamy,
H. B. Singh, G. Wolmershauser and R. J. Butcher, *Organo-
metallics*, 2004, **23**, 4199; (g) A. Panda, S. S. Zade, H. B. Singh
and G. Wolmershauser, *J. Organomet. Chem.*, 2005, **690**,
45 3142; (h) S. Kumar, S. Panda, H. B. Singh, G. Wolmershauser
and R. J. Butcher, *Struct. Chem.*, 2007, **18**, 127.
- 9 (a) C. Santi and T. Wirth, *Tetrahedron: Asymmetry*, 1999, **10**,
1019; (b) T. Wirth, *Angew. Chem., Int. Ed.*, 2000, **39**, 3740.
- 50 10 K. Hiroi, Y. Suzuki and I. Abe, *Tetrahedron: Asymmetry*,
1999, **10**, 1173.
- 11 (a) M. Tiecco, L. Testaferri, C. Santi, C. Tomassini,
F. Marini, L. Bagnoli and A. Temperini, *Tetrahedron: Asym-
metry*, 2000, **11**, 4645; (b) M. Tiecco, L. Testaferri, C. Santi,
C. Tomassini, F. Marini, L. Bagnoli and A. Temperini,
55 *Angew. Chem., Int. Ed.*, 2003, **42**, 3131.
- 12 (a) M. Uchiyama, S. Satoh and A. Ohta, *Tetrahedron Lett.*,
2001, **42**, 1559; (b) M. Uchiyama, M. Hirai, M. Nagata,
R. Katoh, R. Ogawa and A. Ohta, *Tetrahedron Lett.*, 2001, **42**,
4653.
- 13 L. A. Braga, S. J. N. Silva, D. S. Luedtke, R. L. Drekenner,
C. C. Silveira, J. B. T. Rocha and L. A. Wessjohann, *Tetra-
hedron Lett.*, 2002, **43**, 7329.
- 5 14 Y. Miyake, Y. Nishibayashi and S. Uemura, *Bull. Chem. Soc.
Jpn.*, 2002, **75**, 2233.
- 15 T. M. Klapötke, B. Krumm and K. Polborn, *J. Am. Chem.
Soc.*, 2004, **126**, 710.
- 16 (a) M. Kulcsar, A. Silvestru, C. Silvestru, J. E. Drake,
10 C. L. B. MacDonald, M. E. Hursthouse and M. E. Light,
J. Organomet. Chem., 2005, **690**, 3217; (b) M. Kulcsar,
A. Beleaga, C. Silvestru, A. Nicolescu, C. Deleanu,
C. Todasca and A. Silvestru, *Dalton Trans.*, 2007, 2187;
15 (c) A. Beleaga, M. Kulcsar, C. Deleanu, A. Nicolescu,
C. Silvestru and A. Silvestru, *J. Organomet. Chem.*, 2009,
694, 1308; (d) A. Pöllnitz, V. Lippolis, M. Arca and
A. Silvestru, *J. Organomet. Chem.*, 2011, **696**, 2837;
(e) E. Duhamel, A. Pöllnitz, A. Stegărescu and A. Silvestru,
20 *Z. Anorg. Allg. Chem.*, 2011, **637**, 1355; (f) A. Pöllnitz,
C. Silvestru, J.-F. Carpentier and A. Silvestru, *Dalton Trans.*,
2012, **41**, 5060.
- 17 R. Deziel, S. Goulet, L. Grenier, J. Bordeleau and J. Bernier,
J. Org. Chem., 1993, **58**, 3619.
- 25 18 H. Poleschner and K. Seppelt, *Chem.–Eur. J.*, 2004, **10**,
6565.
- 19 S. S. Zade, S. Panda, H. B. Singh, R. B. Sunoj and
R. J. Butcher, *J. Org. Chem.*, 2005, **70**, 3693.
- 30 20 K. Selvakumar, H. B. Singh and R. J. Butcher, *Chem.–Eur.
J.*, 2010, **16**, 10576.
- 21 K. Okamoto, Y. Nishibayashi, S. Uemura and A. Toshimitsu,
Angew. Chem., Int. Ed., 2005, **44**, 3588.
- 22 K. Selvakumar, H. B. Singh, N. Goel, U. P. Singh and
R. J. Butcher, *Dalton Trans.*, 2011, **40**, 9858.
- 35 23 V. P. Singh, H. B. Singh and R. J. Butcher, *Eur. J. Inorg.
Chem.*, 2010, 637 and references therein.
- 24 H. Fujihara, H. Mima and N. Furukawa, *J. Am. Chem. Soc.*,
1995, **117**, 10153.
- 40 25 R. A. Varga, M. Kulcsar and A. Silvestru, *Acta Crystallogr.,
Sect. E: Struct. Rep. Online*, 2010, **66**, o771.
- 26 (a) M. Hall and D. B. Sowerby, *J. Organomet. Chem.*, 1988,
347, 59; (b) W. Clegg, R. J. Errington, G. A. Fisher,
45 D. C. R. Hockless, N. C. Norman, A. G. Orpen and
S. E. Stratford, *J. Chem. Soc., Dalton Trans.*, 1992, 1967;
(c) W. Clegg, R. J. Errington, G. A. Fisher, R. J. Flynn and
N. C. Norman, *J. Chem. Soc., Dalton Trans.*, 1993, 637;
(d) P. Sharma, N. Rosas, A. Toscano, S. Hernandez,
R. Shankar and A. Cabrera, *Main Group Met. Chem.*, 1996,
50 **19**, 21; (e) J. P. H. Charmant, A. G. Orpen, S. C. James,
N. C. Norman and J. Starbuck, *Acta Crystallogr., Sect. E:
Struct. Rep. Online*, 2002, **58**, m488.
- 27 (a) M. Mirbach and M. Wieber, *Gmelin Handbook of
Inorganic Chemistry, Sb Organoantimony Compounds*,
55 Springer-Verlag, Berlin, 1990, Part 5; (b) N. Bertazzi,
T. C. Gibb and N. N. Greenwood, *J. Chem. Soc., Dalton
Trans.*, 1976, 1153; (c) N. Bertazzi, *J. Organomet. Chem.*,

- 1976, **110**, 175; (d) H. J. Breunig and T. Severengiz, *Chem. Zeitung*, 1980, **104**, 202; (e) H. J. Breunig, K. H. Ebert, S. Gülec, M. Dräger, D. B. Sowerby, M. J. Begley and U. Behrens, *J. Organomet. Chem.*, 1992, **427**, 39; (f) H. J. Breunig, M. Denker and E. Lork, *Z. Anorg. Allg. Chem.*, 1999, **625**, 117; (g) H. J. Breunig, T. Koehne, O. Moldovan, A. M. Preda, A. Silvestru, C. Silvestru, R. A. Varga, L. F. Piedra-Garza and U. Kortz, *J. Organomet. Chem.*, 2010, **695**, 1307 and references therein.
- 28 The *N-X-L* nomenclature system has been previously described: *N* valence shell electrons about a central atom *X* with *L* ligands, in: C. W. Perkins, J. C. Martin, A. J. Arduengo III, W. Lau, A. Alegria and K. Kochi, *J. Am. Chem. Soc.*, 1980, **102**, 7753.
- 29 J. Rigaudy and S. P. Klesneym, *IUPAC Nomenclature of Organic Chemistry*, Pergamon Press, Oxford, UK, 1979.
- 30 (a) J. Emsley, *Die Elemente*, Walter de Gruyter, Berlin, 1994; (b) M. Nishio, *Phys. Chem. Chem. Phys.*, 2011, **13**, 13873.
- 31 J. Bordner, G. O. Doak and J. R. Peters Jr., *J. Am. Chem. Soc.*, 1974, **96**, 6763.
- 32 L. M. Opriş, A. Silvestru, C. Silvestru, H. J. Breunig and E. Lork, *Dalton Trans.*, 2003, 4367.
- 33 E. J. Juárez-Pérez, M. C. Aragoni, M. Arca, A. J. Blake, F. A. Devillanova, A. Garau, F. Isaia, V. Lippolis, R. Núñez, A. Pintus and C. Wilson, *Chem.-Eur. J.*, 2011, **17**, 11497.
- 34 The LUMO–HOMO energy gap decreases on going from **2** (4.20 eV) to **4** (3.34 eV), while in the case of the free cation **2a** the energy difference is 5.32 eV.
- 35 (a) R. E. Rundle, *J. Am. Chem. Soc.*, 1947, **69**, 1327; (b) G. Pimentel, *J. Chem. Phys.*, 1951, **19**, 446.
- 36 M. A. Aragoni, M. Arca, F. A. Devillanova, F. Isaia and V. Lippolis, *Cryst. Growth Des.*, 2012, **12**, 2769.
- 37 (a) E. D. Glendening and F. Weinhold, *J. Comput. Chem.*, 1998, **19**, 593; (b) E. D. Glendening and F. Weinhold, *J. Comput. Chem.*, 1998, **19**, 610; (c) E. D. Glendening, J. K. Badenhoop and F. Weinhold, *J. Comput. Chem.*, 1998, **19**, 628.
- 38 According to QTAIM,³⁹ any bonded atoms are connected by a single line, “bond path”, of locally maximum electron density, ρ , that originates a bond critical point (BCP), which represents a minimum of ρ along the bond path. The sign of the Laplacian, $\nabla^2\rho$, of the electron density at a BCP indicates two limit situations: (1) a negative value of $\nabla^2\rho$ indicates a local charge concentration, which means that the interaction is a covalent bond, and (2) a positive value of $\nabla^2\rho$ indicates charge depletion, which means a closed-shell interaction as found in ionic bonds. It is also possible to find positive $\nabla^2\rho$ and relatively high ρ at the BCP, which indicates a covalent polar bond. Another important parameter is the local electronic energy density at BCP, *H*. The sign of *H* indicates whether a charge accumulation at BCP is stabilizing ($H < 0$) or destabilizing ($H > 0$). Thus, a value of $H < 0$ means that the interaction shows a significant covalent contribution and, therefore, a lowering of the potential energy associated with the concentration of charge between the nuclei.⁴⁰ The delocalization index, $\delta(A,B)$, is a measure of the total Fermi correlation shared between the atoms A and B and indicates the extent to which electrons are delocalized over any pair of atoms and allows the determination of a bond order for the A–B bond in which such atoms are connected by a BCP. In the particular case of a formal 3c-4e bond (A–B–C), Molina-Molina and Dobado used the index $\delta(A,C)$ to determine the existence of such a hypervalent bond.⁴¹
- 39 (a) R. Bader, *Atoms in Molecules: A Quantum Theory*, Oxford University Press, USA, 1994; (b) R. Bader, *Chem. Rev.*, 1991, **91**, 893; (c) *The Quantum Theory of Atoms in Molecules*, ed. C. F. Matta and R. J. Boyd, Wiley-VCH Verlag GmbH & Co. KGaA, Weinheim, 2007.
- 40 D. Cremer and E. Kraka, *Angew. Chem., Int. Ed. Engl.*, 1984, **23**, 627.
- 41 J. Molina-Molina and J. A. Dobado, *Theor. Chem. Acc.*, 2001, **105**, 328.
- 42 The ellipticity at the BCP, ϵ , is a measure of the cylindricity of the charge distribution in a bond and, therefore, a measure of the π character in a bond. ϵ values close to zero indicate an axial symmetry (usually a single or triple bond) whereas higher values indicate a partial π character.³⁹
- 43 (a) A. D. Becke and K. E. Edgecombe, *J. Chem. Phys.*, 1990, **92**, 5397; (b) B. Silvi and A. Savin, *Nature*, 1994, **371**, 683.
- 44 (a) W. B. Jensen, *Chem. Ed.*, 2006, **83**, 1751; (b) P. v. R. Schleyer, *Chem. Eng. News*, 1984, **62**, 4; (c) D. W. Smith, *J. Chem. Educ.*, 2008, **82**, 1202; (d) R. J. Gillespie and E. A. Robinson, *Inorg. Chem.*, 1995, **34**, 978.
- 45 E. Espinosa, E. Molins and C. Lecomte, *Chem. Phys. Lett.*, 1998, **285**, 170.
- 46 P. N. Jayaram, G. Roy and G. Mugesh, *J. Chem. Sci.*, 2008, **120**, 143.
- 47 MestReC and MestReNova, Mestrelab Research S.L., A Coruña 15706, Santiago de Compostela.
- 48 Y. Yamamoto, X. Chen, S. Kojima, K. Ohdoi, M. Kitano, Y. Doi and K.-y. Akiba, *J. Am. Chem. Soc.*, 1995, **117**, 3922.
- 49 G. Becker, O. Mundt, M. Sachs, H. J. Breunig, E. Lork, J. Probst and A. Silvestru, *Z. Anorg. Allg. Chem.*, 2001, **627**, 699.
- 50 T. T. Bamgboye, M. J. Begley and D. B. Sowerby, *J. Organomet. Chem.*, 1989, **362**, 77.
- 51 C. J. Carmalt, A. H. Cowley, R. D. Culp, R. A. Jones, S. Kamepalli and N. C. Norman, *Inorg. Chem.*, 1997, **36**, 2770.
- 52 G. M. Sheldrick, *Acta Crystallogr., Sect. A: Fundam. Crystallogr.*, 2008, **64**, 112.
- 53 *DIAMOND – Visual Crystal Structure Information System*, Crystal Impact, Postfach 1251, D-53002 Bonn, Germany, 2001.
- 54 M. J. Frisch, G. W. Trucks, H. B. Schlegel, G. E. Scuseria, M. A. Robb, J. R. Cheeseman, G. Scalmani, V. Barone, B. Mennucci, G. A. Petersson, H. Nakatsuji, M. Caricato, X. Li, H. P. Hratchian, A. F. Izmaylov, J. Bloino, G. Zheng, J. L. Sonnenberg, M. Hada, M. Ehara, K. Toyota, R. Fukuda, J. Hasegawa, M. Ishida, T. Nakajima, Y. Honda, O. Kitao, H. Nakai, T. Vreven, J. J. A. Montgomery, J. E. Peralta,

- 1 F. Ogliaro, M. Bearpark, J. J. Heyd, E. Brothers, K. N. Kudin, V. N. Staroverov, R. Kobayashi, J. Normand, K. Raghavachari, A. Rendell, J. C. Burant, S. S. Iyengar, J. Tomasi, M. Cossi, N. Rega, J. M. Millam, M. Klene, J. E. Knox, J. B. Cross, V. Bakken, C. Adamo, J. Jaramillo, R. Gomperts, R. E. Stratmann, O. Yazyev, A. J. Austin, R. Cammi, C. Pomelli, J. W. Ochterski, R. L. Martin, K. Morokuma, V. G. Zakrzewski, G. A. Voth, P. Salvador, J. J. Dannenberg, S. Dapprich, A. D. Daniels, Ö. Farkas, J. B. Foresman, J. V. Ortiz, J. Cioslowski and D. J. Fox, Gaussian Inc., Wallingford CT, 2010.
- 55 C. Adamo and V. Barone, *J. Chem. Phys.*, 1998, **108**, 664.
- 56 A. Schafer, H. Horn and R. Ahlrichs, *J. Chem. Phys.*, 1992, **97**, 2571.
- 15 57 W. R. Wadt and P. J. Hay, *J. Chem. Phys.*, 1985, **82**, 284.
- 58 C. E. Check, T. O. Faust, J. M. Bailey, B. J. Wright, T. M. Gilbert and L. S. Sunderlin, *J. Phys. Chem. A*, 2001, **105**, 8111.
- 20 59 E. D. Glendening, J. K. Badenhop, A. E. Reed, J. E. Carpenter, J. A. Bohmann, C. M. Morales and F. Weinhold, *NBO 5.0*, Theoretical Chemistry Institute, University of Wisconsin, Madison, WI, 2001, <http://www.chem.wisc.edu/~nbo5>
- 60 T. A. Keith, *AIMAll (Version 11.10.16)*, TK Gristmill Software, Overland Park, KS, USA, 2011, aim.tkgristmill.com
- 61 (a) X. Gironés, R. Ponec and J. Roithova, *WBader v.1.0*, Prague, 2000; (b) R. Ponec and X. Gironés, *J. Phys. Chem. A*, 2002, **106**, 9506.
- 62 T. Lu and F. Chen, *J. Comput. Chem.*, 2012, **33**, 580.
- 63 T. A. Keith and M. J. Frisch, *J. Phys. Chem. A*, 2011, **115**, 12879.
- 10 64 S. Noury, X. Krokidis, F. Fuster and B. Silvi, *TopMod package*, Laboratoire de Chimie Theorique, Universite Pierre et Marie Curie, Paris, 1997, available at http://www.lct.jussieu.fr/pagesperso/silvi/topmod_english.html
- 15 65 S. Noury, X. Krokidis, F. Fuster and B. Silvi, *Comput. Chem. Eng.*, 1999, **23**, 597.
- 66 S. Portmann, *Molekel, Linux Version 4.3.11*, Nov. 2002.
- 67 A.-R. Allouche, *J. Comput. Chem.*, 2011, **32**, 174.
- 20 68 *The PyMOL Molecular Graphics System, Version 1.2r2*, Schrödinger, LLC, <http://pymol.org/>
- 25
- 30
- 35
- 40
- 45
- 50
- 55